Am J Transl Res 2018;10(10):3053-3067
www.ajtr.org /ISSN:1943-8141/AJTR0076837

Original Article

Inducible pluripotent stem cell-derived mesenchymal stem cell therapy effectively protected kidney from acute ischemia-reperfusion injury

Sheung-Fat Ko[1], Yen-Ta Chen[2,10], Christopher Glenn Wallace[7], Kuan-Hung Chen[3], Pei-Hsun Sung[4], Ben-Chung Cheng[5], Tien-Hung Huang[4,9], Yi-Ling Chen[4,9], Yi-Chen Li[4], Hsueh-Wen Chang[8], Mel S Lee[6], Chih-Chao Yang[5*], Hon-Kan Yip[4,9,10,11,12*]

[1]Department of Radiology, [2]Division of Urology, Department of Surgery, [3]Department of Anesthesiology, [4]Division of Cardiology, Department of Internal Medicine, [5]Division of Nephrology, Department of Internal Medicine, [6]Department of Orthopedics, Kaohsiung Chang Gung Memorial Hospital and Chang Gung University College of Medicine, Kaohsiung 83301, Taiwan; [7]Department of Plastic Surgery, University Hospital of South Manchester, Manchester, UK; [8]Department of Biological Sciences, National Sun Yat-sen University, Kaohsiung 80424, Taiwan; [9]Institute for Translational Research in Biomedicine, [10]Center for Shockwave Medicine and Tissue Engineering, Kaohsiung Chang Gung Memorial Hospital, Kaohsiung 83301, Taiwan; [11]Department of Medical Research, China Medical University Hospital, China Medical University, Taichung 40402, Taiwan; [12]Department of Nursing, Asia University, Taichung 41354, Taiwan. [*]Equal contributions.

Received March 27, 2018; Accepted September 5, 2018; Epub October 15, 2018; Published October 30, 2018

Abstract: This study tested whether inducible pluripotent stem cell (iPSC)-derived mesenchymal stem cell (MSC) therapy could effectively protect kidney from acute ischemia (1 h) - reperfusion (5 day) injury (IRI). Male-adult SD-rats (n = 24) were equally categorized into groups 1 (sham-control), 2 [sham-control + iPSC-MSC (1.2×10^6 cells/rat)], 3 (IR only) and 4 (IR + iPSC-MSC). Blood urine nitrogen/creatinine levels and ratio of urine protein to creatinine, kidney weight and expressions of inflammation (TNF-α/NF-κB), oxidative-stress (NOX-1/NOX-2/oxidized protein) and apoptosis (mitochondrial-Bax/cleaved caspase-3/PARP) were significantly higher in group 3 than in groups 1, 2 and 4 and significantly higher in group 4 than in groups 1 and 2 (all P<0.0001), but showed no differences between groups 1 and 2, whereas the protein expressions of anti-inflammation (IL-4/IL-10) and endothelial (CD31/vWF) markers exhibited an opposite pattern to inflammation among the four groups (all P<0.0001). Protein expressions of angiogenesis (VEGF/CXCR4/SDF-1α) markers progressively increased from groups 1 to 4 (all P<0.0001). Cellular expressions of kidney injury score/DNA-damage (γ-H2AX)/apoptotic nuclei and glomerulus-tubular-damage (KIM/FSP-1) displayed an identical pattern to inflammation, whereas the cellular expressions of glomerulus-tubular-integrity (dystroglycan/podocin/p-cadherin/synaptopodin/ZO-1/fibronectin) revealed an opposite pattern to inflammation among the four groups (all P<0.0001). In conclusion, iPSC-derived MSC therapy effectively protected kidney against IRI.

Keywords: Inducible pluripotent stem cell, mesenchymal stem cell, acute kidney ischemia reperfusion injury, inflammation, oxidative stress

Introduction

Whilst the kidneys are physiologically critical to electrolyte, water and pH homeostasis and to detoxification and excretion of toxins and drug metabolites, they are also vulnerable to acute kidney injury (AKI). AKI is common and is an independent predictor of morbidity and mortality in patients hospitalized for any disease entity [1-5]. AKI can have several etiologies, such as from cardiac surgery [6-8], burns [5], drugs [3], myocardial infarction [4], catheter-based interventions [9, 10], post-transplantation procedures [11], sepsis [12] and ischemia-reperfusion injury (IRI) [13, 14]. Of these, acute kidney IRI (AK-IRI) is common, causes unacceptably high inpatient morbidity and mortality [1, 4-7], lacks effective treatments and is therefore an important clinical problem to be solved [1, 13, 15, 16].

The mechanisms underlying AK-IRI are mainly increased oxidative stress, pro-inflammatory cytokines, inflammatory reaction and cellular

apoptosis, as well as inappropriate immune responses after prolonged or even transient IRI [17-20]. Accordingly, a single pharmaceutical intervention is unlikely to abrogate AK-IRI or its effects, raising the need for investigating alternative innovative strategies.

Mesenchymal stem cells (MSCs), especially adipose-derived MSCs, have intrinsic capacity to alleviate inflammation [20-24] and suppress innate and adaptive immunity [20-26] through reducing immunogenicity [20-27]. In experimental and clinical trials, MSC therapy effectively improved ischemia-related organ dysfunction [18, 20, 21, 24] and clinical outcome for patients with severe immunological disorders [26]. Furthermore, with the advent of reprogramming technology, human inducible pluripotent stem cells (iPSCs) have practically unlimited proliferation potential and the capability to differentiate into any cell type, providing a potential source of tissue-specific progenitors for cell therapy [27-31]. Therefore, iPSCs may be unique tissue regenerative contributors with greater potential than MSCs for developing donor-specific personalized cell replacement therapies [32] for various disease entities, including AKI/AK-IRI.

Materials and methods

Ethics

All animal experimental procedures were approved by the Institute of Animal Care and Use Committee at Kaohsiung Chang Gung Memorial Hospital (Affidavit of Approval of Animal Use Protocol No. 2016092910) and performed in accordance with the Guide for the Care and Use of Laboratory Animals [The Eighth Edition of the Guide for the Care and Use of Laboratory Animals (NRC 2011)].

Animals were housed in an Association for Assessment and Accreditation of Laboratory Animal Care International (AAALAC)-approved animal facility in our hospital with controlled temperature and light cycle (24°C and 12/12 light cycle).

Animal grouping, procedure and protocol for AK-IRI and treatment strategy

Pathogen-free, adult male Sprague-Dawley (SD) rats (n = 24) weighing 320-350 g (Charles River Technology, BioLASCO Taiwan Co. Ltd., Taiwan) were equally categorized into four groups (i.e., n = 6 per group): Sham control (SC) (laparotomy only), SC + iPSC-derived mesenchymal stem cell (MSC) (iPSC-MSC) (1.2×10^6 cells by intravenous administration 3 h after laparotomy), IRI only, and IRI + iPSC-MSC (1.2×10^6 cells by intravenous administration 3 h after IR procedure).

The AK-IRI procedure and protocol have previously been described [18, 20]. Briefly, animals in groups 1 to 4 were anesthetized by inhalational 2.0% isoflurane and placed supine on a warming pad at 37°C for midline laparotomies. SC animals underwent laparotomy only, while AK-IRI of both kidneys were induced in all animals in groups 3 and 4 by clamping the renal pedicles for one hour using non-crushing vascular clips. The animals in each group were sacrificed and kidney specimens harvested for individual study by day 5 after the AK-IRI procedure. The dosage and time points of iPSC administration to the animals at 3 h after AK-IRI were based on our recent reports [18, 20].

Assessment of time courses of circulating levels of creatinine and BUN at days 0, 3 and 5, and collection of 24-hour urine for the ratio of urine protein to creatinine at 72 h after AK-IRI

Blood samples were drawn from all animals in each group to assess changes in serum creatinine and blood urine nitrogen (BUN) levels at baseline and days 3 and 5 after AK-IRI procedure.

For the collection of 24-hr urine, for individual study, each animal was put into a metabolic cage [DXL-D, space: 19 × 29 × 55 cm, Suzhou Fengshi Laboratory Animal Equipment Co. Ltd., Mainland China] for 24 h with free access to food and water. Urine in 24 h was collected in all animals from 48 to 72 h after the AK-IRI procedure to determine daily urine volume and the ratio of urine protein to creatinine.

Qualitative analysis of kidney injury scores at day 5 after AK-IRI procedure

Histopathology scoring of kidney injury was assessed in a blinded fashion as previously reported [18, 20]. Briefly, kidney specimens from all animals were fixed in 10% buffered formalin, embedded in paraffin, sectioned at 5 μm and stained with hematoxylin and eosin (H&E) for light microscopy. The scoring system reflected the grading of tubular necrosis, loss of brush border, cast formation, and tubular dilatation in 10 randomly chosen, non-overlapping fields

(200 ×), as follows: 0 (none), 1 (≤ 10%), 2 (11-25%), 3 (26-45%), 4 (46-75%), and 5 (≥ 76%).

Western blot analysis

The procedure and protocol for Western blot analysis have been described in our previous reports [18, 20-24]. Briefly, equal amounts (50 μg) of protein extracts were loaded and separated by SDS-PAGE using acrylamide gradients. After electrophoresis, the separated proteins were transferred electrophoretically to a polyvinylidene difluoride (PVDF) membrane (GE, UK). Nonspecific sites were blocked by incubation of the membrane in blocking buffer [5% nonfat dry milk in T-TBS (TBS containing 0.05% Tween 20)] overnight. The membranes were incubated with the indicated primary antibodies [mitochondrial Bax (1:1000, Abcam, Cambridge, MA, USA), cleaved caspase 3 (1:1000, Cell Signaling, Danvers, MA, USA), cleaved Poly (ADP-ribose) polymerase (PARP) (1:1000, Cell Signaling, Danvers, MA, USA), NOX-1 (1:1500, Sigma, St. Louis, Mo, USA), NOX-2 (1:750, Sigma, St. Louis, Mo, USA), mitochondrial Bax (1:1000, Abcam, Cambridge, MA, USA), tumor necrosis factor (TNF)-α (1:1000, Cell Signaling, Danvers, MA, USA), nuclear factor (NF)-κB (1:600, Abcam, Cambridge, MA, USA), interleukin (IL)-4 (1:1000, Abcam, Cambridge, MA, USA), IL-10 (1:1000, Abcam, Cambridge, MA, USA), CD31 (1:1000, Abcam, Cambridge, MA, USA), von Willebrand factor (vWF) (1:1000, Abcam, Cambridge, MA, USA), stromal cell-derived factor (SDF)-1α (1:1000, Cell Signaling, Danvers, MA, USA), CXCR4 (1:1000, Abcam, Cambridge, MA, USA), vascular endothelial growth factor (VEGF) (1:1000, Abcam, Cambridge, MA, USA), and actin (1:6000, Chemicon, Billerica, MA, USA)] for 1 hour at room temperature. Horseradish peroxidase-conjugated anti-rabbit immunoglobulin IgG (1:2000, Cell Signaling, Danvers, MA, USA) was used as a secondary antibody for one-hour incubation at room temperature. The washing procedure was repeated eight times within one hour. Immunoreactive bands were visualized by enhanced chemiluminescence (ECL; Amersham Biosciences, Amersham, UK) and exposed to Biomax L film (Kodak, Rochester, NY, USA). For quantification, ECL signals were digitized using Labwork software (UVP, Waltham, MA, USA).

Immunohistochemical (IHC) and immunofluorescent (IF) staining

The procedure and protocol for IHC and IF staining have been described in our previous reports [18, 20-24]. For IHC and IF staining, rehydrated paraffin sections were first treated with 3% H_2O_2 for 30 minutes and incubated with Immuno-Block reagent (BioSB, Santa Barbara, CA, USA) for 30 minutes at room temperature.

Sections were then incubated with primary antibodies specifically against zonula occludens-1 (ZO-1) (1:500, Novus), kidney injury molecule (KIM)-1 (1:500, R&D system), fibroblast specific protein (FSP)-1 (1:200, Abcam), P-cadherin (1:200, Novus), snail (1:500, Abcam), podocin (1:50, Abcam), dystroglycan (1:50, Abcam), fibronectin (1:200, Abcam), synaptopodin (1:500, Santa Cruz) TUNEL assay (In Situ Cell Death Detection Kit, Fluorescein, Roche), γ-H2AX (1:500, Abcam), while sections incubated with the use of irrelevant antibodies served as controls. Three sections of kidney specimen from each rat were analyzed. For quantification, three random HPFs (200 × or 400 × for IHC and IF studies) were analyzed in each section. The mean number of positively-stained cells per HPF for each animal was then determined by summation of all numbers divided by 9.

An IHC-based/IF-based scoring system was adopted for semi-quantitative analyses of ZO-1, synaptopodin, podocin, dystroglycan, P-cadherin, KIM-1 and FSP-1 in the kidneys as a percentage of positive cells in blinded fashion (score of positively-stained cell for these biomarkers as: 0 = negative staining; 1 ≤ 15%; 2 = 15-25%; 3 = 25-50%; 4 = 50-75%; 5 ≥ 75%-100%/per HPF).

Assessment of oxidative stress

The procedure and protocol for evaluating the protein expression of oxidative stress have been described in our previous reports [18, 20-24]. The Oxyblot Oxidized Protein Detection Kit was purchased from Chemicon, Billerica, MA, USA (S7150). DNPH derivatization was carried out on 6 μg of protein for 15 minutes according to the manufacturer's instructions. One-dimensional electrophoresis was carried out on 12% SDS/polyacrylamide gel after DNPH derivatization. Proteins were transferred to nitrocellulose membranes that were then incubated in the primary antibody solution (anti-DNP 1:150) for 2 hours, followed by incubation in secondary antibody solution (1:300) for 1 hour at room temperature. The washing proce-

dure was repeated eight times within 40 minutes. Immunoreactive bands were visualized by enhanced chemiluminescence (ECL; Amersham Biosciences, Amersham, UK) which was then exposed to Biomax L film (Kodak, Rochester, NY, USA). For quantification, ECL signals were digitized using Labwork software (UVP, Waltham, MA, USA). For oxyblot protein analysis, a standard control was loaded on each gel.

In vitro study of cell culturing for differentiation of human iPSC into MSCs (Supplementary Figure 1)

The procedure and protocol of human iPSC culture for differentiation into MSCs were as per the manufacturer's instructions. By day 1, human iPSCs [mTeSR™1; StemCell, #28315) were first washed by 5 mL PBS, followed by 2 mL Accutase (Gibco, #A1110501; Accutase: PBS = 1:1); the incubator reaction continued for 1 min. Then 2 mL KO DMEM/F12 (Gibco, #12660012) was added and the cells were collected in 15 mL centrifuge tubes for 5 mins centrifuge (× 200 g). The cells were then cultured in a 10 cm dish for 24 h in mTeSR™1 culture medium.

By day 2, the cells (mTeSR™1) were collected and washed by 5 mL PBS. STEMdiff™-ACF Mesenchymal Induction Medium (StemCell, #05241) was added and then incubator culture proceeded for 24 h. The STEMdiff™-ACF Mesenchymal Induction Medium was exchanged once/day from days 1 to 3. This procedure was repeated on days 3 to 6. On days 7 to 21, the procedure was repeated but the culture medium was refreshed every 3 alternative days.

Human iPSC-derived MSCs were instructed to differentiate into adipocytes, chondrocytes, and osteoblasts (Supplementary Figure 2)

For differentiation of adipocytes, chondrocytes, and osteocytes, human iPSC-derived MSCs were cultured in MesenCult™ Adipogenic (StemCell, #05412; 21 days culture), Chondrogenic (StemCell, #05455; 21 days culture), and Osteogenic (StemCell, #05465; 15 days culture) differentiation medium, respectively, exchanging culture media once every 3 days.

Statistical analysis

Quantitative data are expressed as mean ± SD. Statistical analysis was adequately performed by ANOVA followed by Bonferroni multiple-comparison post hoc test. Statistical analysis was performed using SPSS statistical software for Windows version 22 (SPSS for Windows, version 22; SPSS, IL, U.S.A.). A value of $P<0.05$ was considered as statistically significant.

Results

Human iPSC differentiated into MSCs and MSCs differentiated into adipocytes, chondrocytes and osteocytes (Supplementary Figures 1 and 2)

As per the manufacturer's instructors, plentiful MSCs were found in the culture discs (Supplementary Figure 1). Flow cytometry demonstrated that the typical MSC surface markers were identified by 21-day culturing, implicating that human iPSCs were successfully differentiated into MSCs (Supplementary Figure 1).

To determine whether iPSC-derived MSCs differentiated into adipocytes, osteocytes and chondrocytes, iPSC-derived MSCs were cultured in three culture media that were specific for these three different cell types. The results showed that iPSC-derived MSCs had successfully differentiated into adipocytes, osteocytes and chondrocytes, respectively (Supplementary Figure 2).

*Time courses of circulating levels of creatinine and BUN, ratios of urine protein to creatinine and at day 3, and total left and right kidney weight and histopathological findings of kidney injury score at day 5 after AK-IRI procedure (**Figure 1**)*

Prior to the IR procedure, the serum levels of creatinine and BUN did not differ among the four groups. However, by day 3 after the IR procedure, the serum levels of creatinine and BUN were significantly higher in group 3 (IRI) than in group 1 (SC), group 2 (SC + iPSC-MSC) and group 4 (IRI + iPSC-MSC), significantly higher in group 4 than in groups 1 and 2, and not significantly different between groups 1 and 2. By day 5 after IR procedure, these two parameters expressed similar pattern to day 3, but they showed no difference among groups 1, 2 and 4. The ratio of urine protein to urine creatinine (i.e., 24 h urine to be collected from 48 h to 72 after IR procedure) was significantly higher in group 3 than in groups 1, 2 and 4, but showed no difference among the latter three groups. The total weight of the right and left kidneys exhibited an identical pattern to the day-5 creatinine level among the four groups. These find-

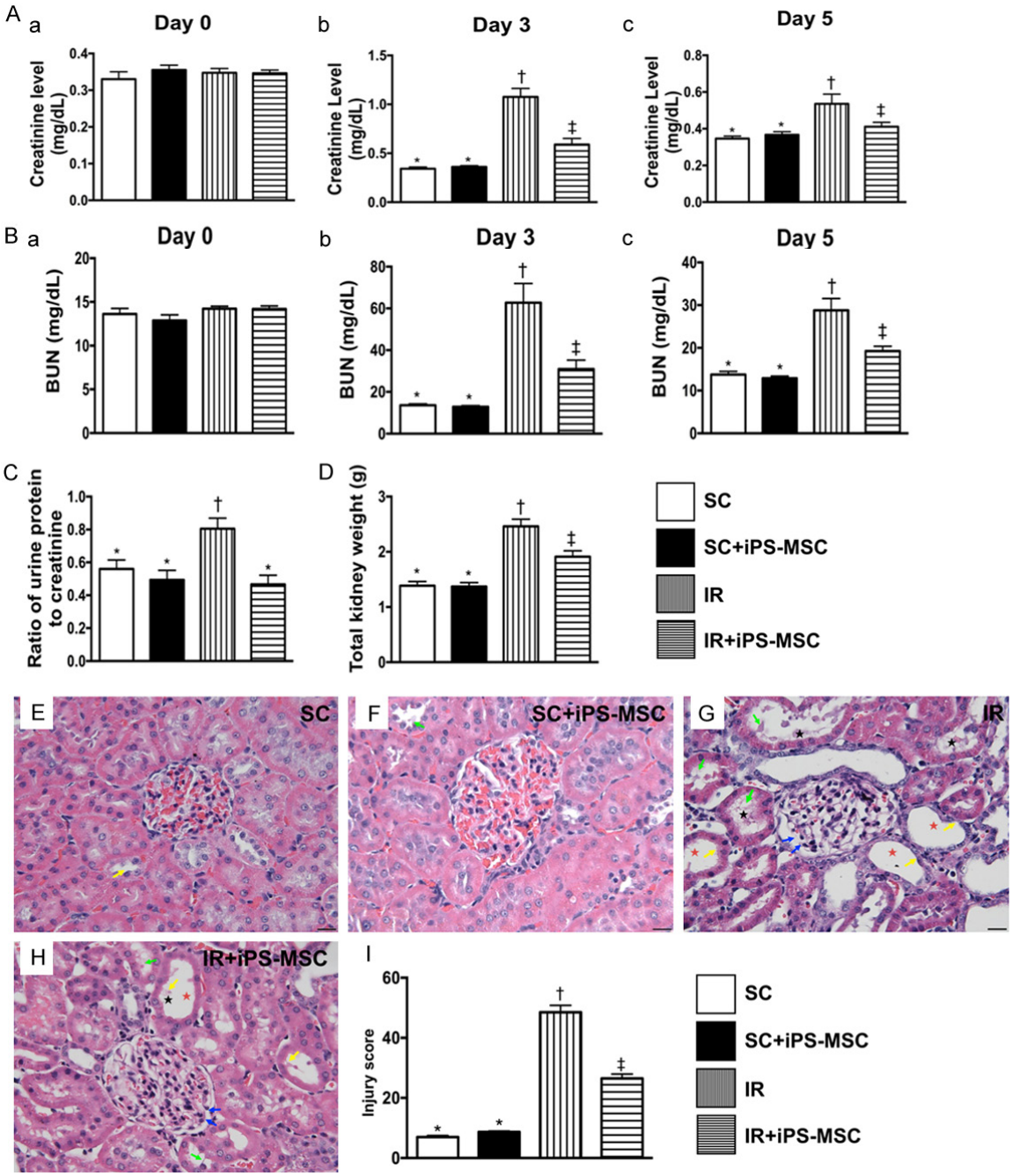

Figure 1. Serial changes of circulating levels of creatinine and BUN, ratios of urine protein to creatinine and at day 3, and total left and right kidney weight and histopathological findings of kidney injury score at day 5 after AK-IRI procedure. (A) Time courses of circulating levels of creatinine: (a) prior to IR procedure, P>0.5; (b) by day 3 after IR procedure, * vs. other groups with different symbols (†, ‡), P<0.001; (c) by day 5 after IR procedure, * vs. †, P<0.001. (B) Time courses of circulating levels of blood urea nitrogen (BUN): (a) prior to IR procedure, P>0.5; (b) by day 3 after IR procedure, * vs. other groups with different symbols (†, ‡); (c) by day 5 after IR procedure, * vs. other groups with different symbols (†, ‡). (C) Ratio of urine protein to urine creatinine by day 3 after IR procedure, * vs. †, P<0.01. (D) The total kidney weight (i.e., combined left and right kidney) at day 5 after IR procedure, * vs. other groups with different symbols (†, ‡). (E-H) Light microscopic findings (400 ×; H&E stain) showing significantly higher loss of brush border in renal tubules (yellow arrows), tubular necrosis (green arrows), tubular dilatation (red asterisk) protein cast formation (black asterisk), and dilatation of Bowman's capsule (blue arrows) in IR group than in other groups. (I) Analytical result of kidney injury score, * vs. other groups with different symbols (†, ‡), P<0.0001. Scale bars in right lower corner represent 20 μm. All statistical analyses were performed by one-way ANOVA, followed by Bonferroni multiple comparison post hoc test (n = 6 for each group). Symbols (*, †, ‡) indicate significance (at 0.05 level). SC = sham control; IR = ischemia reperfusion; iPS-MSC = human inducible pluripotent stem cell-derived mesenchymal stem cell.

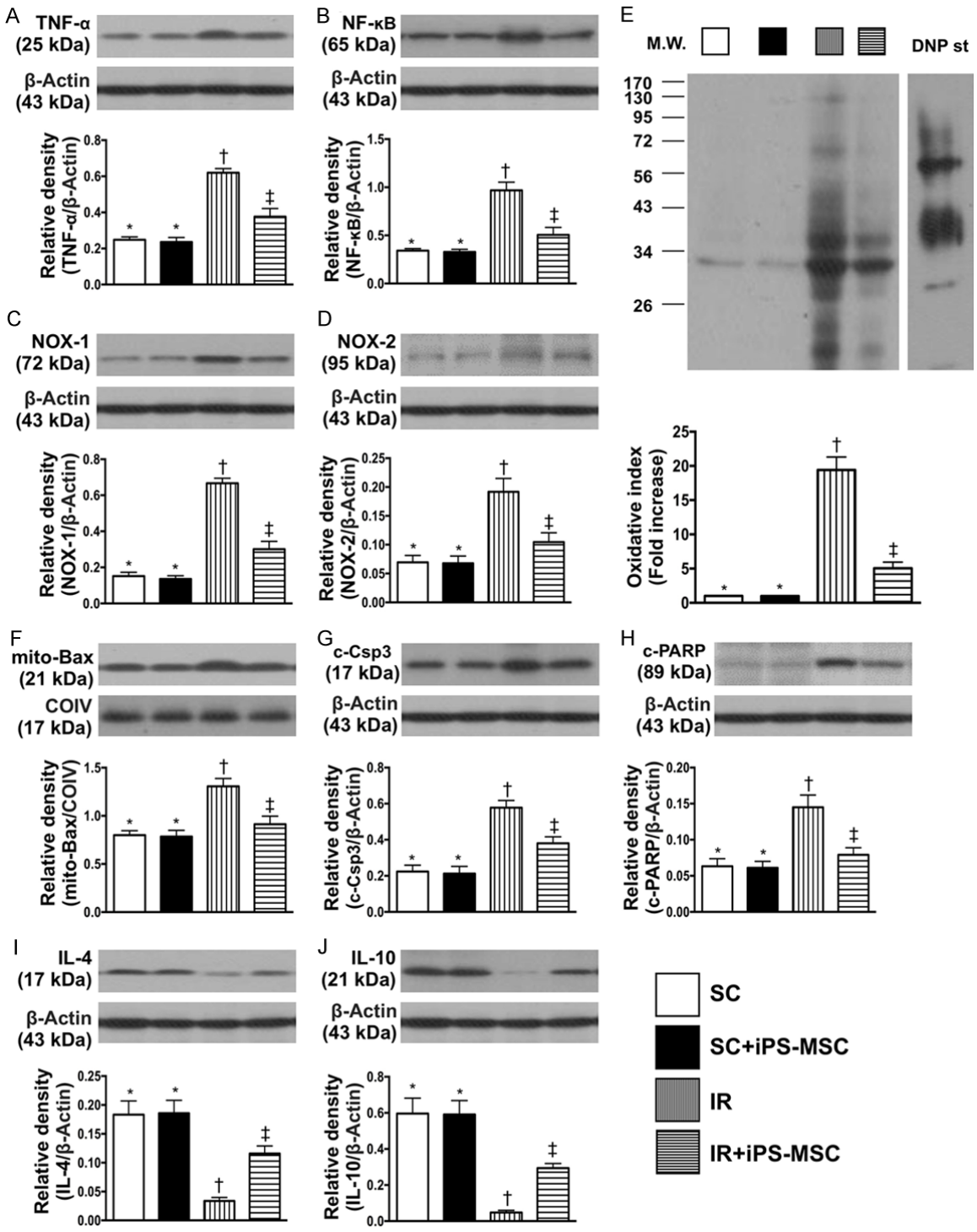

Figure 2. Protein expressions of inflammation, oxidative stress, apoptosis and anti-inflammation at day 5 after IR procedure. A. Protein expression of tumor necrosis factor (TNF)-α, * vs. other groups with different symbols (†, ‡), P<0.001. B. Protein expression of nuclear factor (NF)-κB, * vs. other groups with different symbols (†, ‡), P<0.0001. C. Protein expression of NOX-1, * vs. other groups with different symbols (†, ‡), P<0.0001. D. Protein expression of NOX-2, * vs. other groups with different symbols (†, ‡), P<0.0001. E. Oxidized protein expression, * vs. other groups with different symbols (†, ‡), P<0.0001. (Note: left and right lanes shown on the upper panel represent protein molecular weight marker and control oxidized molecular protein standard, respectively). M.W = molecular weight; DNP = 1-3 dinitrophenylhydrazone. F. The protein expressions of mitochondrial (mito)-Bax, * vs. other groups with different symbols (†, ‡), P<0.001. G. Protein expression of cleaved caspase 3 (c-Csp3), * vs. other groups with different symbols (†, ‡), P<0.001. H. Protein expression of cleaved Poly (ADP-ribose) polymerase (c-PARP), * vs. other groups with different symbols (†, ‡), P<0.001. I. Protein expression of interleukin (IL)-4, * vs. other groups with different

symbols (†, ‡), P<0.0001. J. Protein expression of IL-10, * vs. other groups with different symbols (†, ‡), P<0.0001. All statistical analyses were performed by one-way ANOVA, followed by Bonferroni multiple comparison post hoc test (n = 6 for each group). Symbols (*, †, ‡) indicate significance (at 0.05 level). SC = sham control; IR = ischemia reperfusion; iPS-MSC = human inducible pluripotent stem cell-derived mesenchymal stem cell.

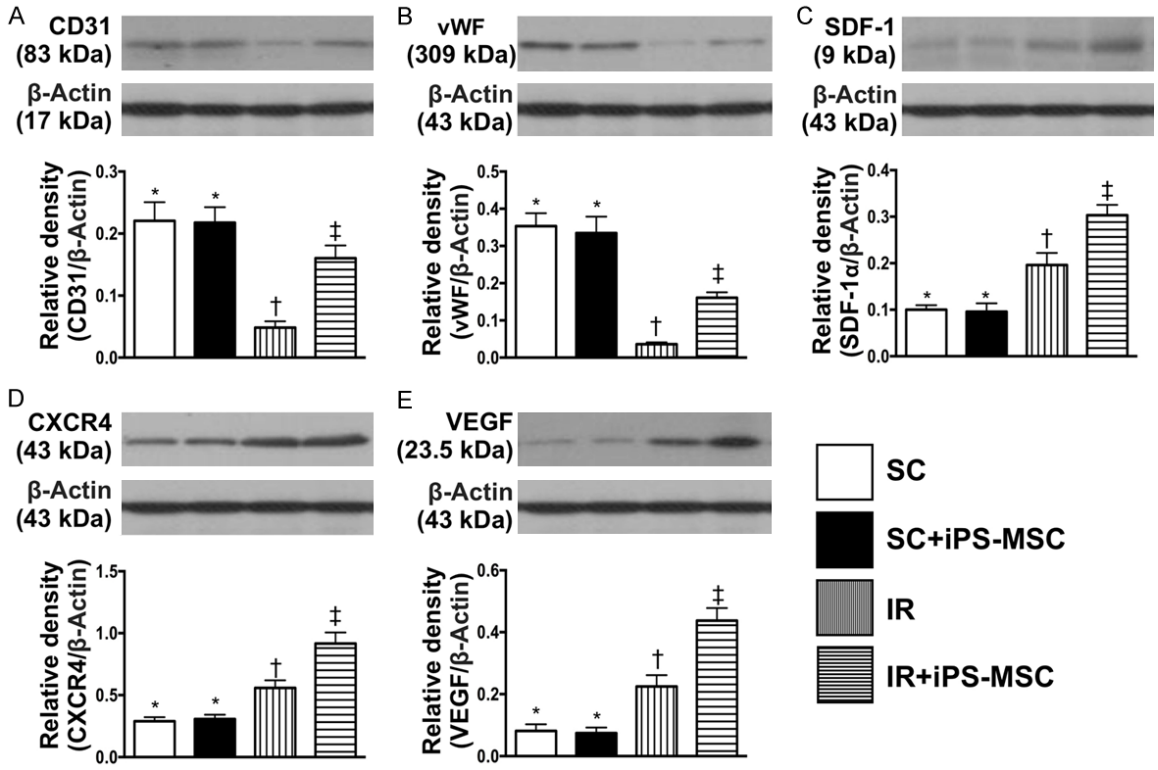

Figure 3. Protein expressions of endothelial and angiogenesis biomarkers at day 5 after IR procedure after IR procedure. A. Protein expressions of CD31, * vs. other groups with different symbols (†, ‡), P<0.0001. B. Protein expression of von Willebrand factor (vWF), * vs. other groups with different symbols (†, ‡), P<0.0001. C. Protein expressions of stromal cell-derived factor (SDF)-1α, * vs. other groups with different symbols (†, ‡), P<0.0001. D. Protein expression of CXCR4, * vs. other groups with different symbols (†, ‡), P<0.0001. E. Protein expression of vascular endothelial growth factor (VEGF), * vs. other groups with different symbols (†, ‡), P<0.0001. All statistical analyses were performed by one-way ANOVA, followed by Bonferroni multiple comparison post hoc test (n = 6 for each group). Symbols (*, †, ‡) indicate significance (at 0.05 level). SC = sham control; IR = ischemia reperfusion; iPS-MSC = human inducible pluripotent stem cell-derived mesenchymal stem cell.

ings suggest that human iPSC-derived MSC therapy effectively protected against AK-IRI.

H&E microscopy showed that the kidney injury score was significantly higher in group 3 than in groups 1, 2 and 4 and significantly higher in group 4 than in groups 1 and 2, but it was not different between groups 1 and 2. These findings again suggest human iPSC-derived MSC therapy effectively protected against AK-IRI.

*Protein expressions of inflammation, oxidative stress, apoptosis and anti-inflammation at day 5 after IR procedure (**Figure 2**)*

The protein expressions of TNF-α and NF-κB, two indicators of inflammation, were significantly higher in group 3 than in groups 1, 2 and 4, and significantly higher in group 4 than in groups 1 and 2, but not different between groups 1 and 2. Protein expressions of NOX-1, NOX-2 and oxidized protein, three indicators of oxidative stress, exhibited a similar pattern to inflammation among the four groups.

The protein expressions of mitochondrial Bax, cleaved caspase 3 and cleaved PARP, three indicators of apoptosis, were significantly higher in group 3 than in other groups, significantly higher in group 4 than in groups 1 and 2, and similar between groups 1 and 2. On the other hand, the protein expressions of IL-4 and IL-10, two indicators of anti-inflammation, exhibited an opposite pattern to apoptosis among the four groups.

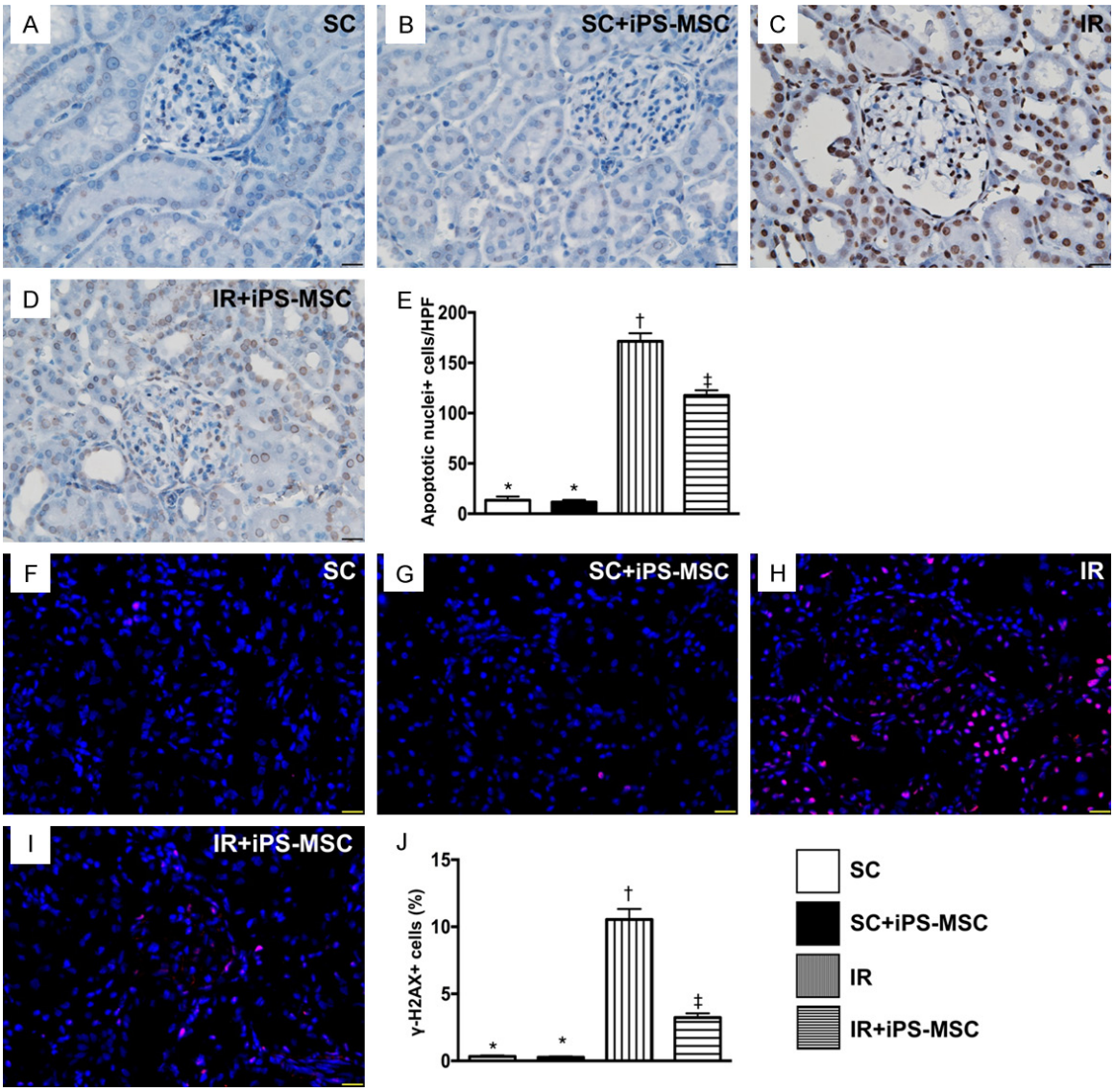

Figure 4. Cellular expressions of apoptotic and DNA-damaged markers in kidney parenchyma at day 5 after IR procedure. A-D. Illustrating the microscopic finding (400 ×) of TUNEL assay for identification of apoptotic nuclei (gray color). E. Analytical result of apoptotic nuclei, * vs. other groups with different symbols (†, ‡), P<0.0001. F-I. Showing the immunofluorescent microscopic finding (400 ×) for identification of γ-H2X+ cell (pink color). J. Analytical result of number of γ-H2X+ cells, * vs. other groups with different symbols (†, ‡), P<0.0001. Scale bars in right lower corner represent 20 μm. All statistical analyses were performed by one-way ANOVA, followed by Bonferroni multiple comparison post hoc test (n = 6 for each group). Symbols (*, †, ‡) indicate significance (at 0.05 level). HPFs = high-power field; SC = sham control; IR = ischemia reperfusion; iPS-MSC = human inducible pluripotent stem cell-derived mesenchymal stem cell.

*Protein expressions of endothelial and angiogenesis biomarkers at 72 h after AK-IRI procedure (**Figure 3**)*

The protein expressions of CD31 and vWF, two endothelial cell biomarkers, were significantly lower in group 3 than in other groups, significantly lower in group 4 than in groups 1 and 2, and similar between groups 1 and 2. Protein expressions of SDF-1α, CXCR4 and VEGF significantly and progressively increased from groups 1 and 2 to 4, suggesting in intrinsic response to IRI, enhanced by human iPSC-derived MSC therapy.

*Cellular expressions of apoptotic and DNA-damage markers in kidney parenchyma at 72 h after AK-IRI procedure (**Figure 4**)*

The IHC microscopic TUNEL assay showed that the number of apoptotic nuclei was significantly

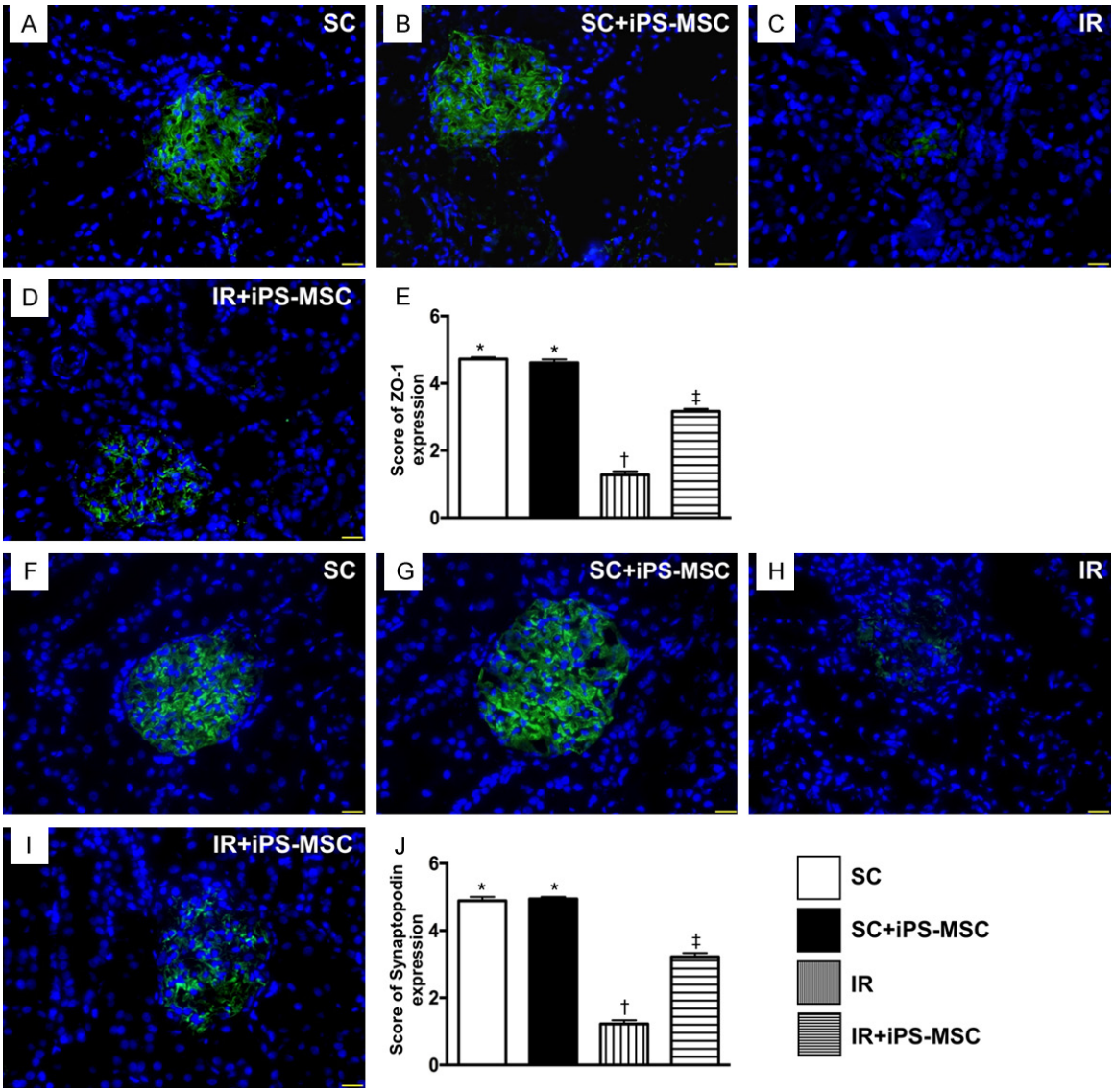

Figure 5. Identification of the expressions of ZO-1 and synaptopodin in glomeruli at day 5 after IR procedure. A-D. Immunofluorescent (IF) microscopic finding (400 ×) for identification of the expression of positively-stained ZO-1 in glomeruli (green color). E. Analytical results of ZO-1 expression, * vs. other groups with different symbols (*, †, ‡), P<0.0001. F-I. IF microscopic finding (400 ×) for identification of expression of positively-stained synaptopodin in glomeruli (green color). J. Analytical results of synaptopodin expression, * vs. other groups with different symbols (*, †, ‡), P<0.0001. Scale bars in right lower corner represent 20 μm. All statistical analyses were performed by one-way ANOVA, followed by Bonferroni multiple comparison post hoc test (n = 6 for each group). Symbols (*, †, ‡) indicate significance (at 0.05 level). SC = sham control; IR = ischemia reperfusion; iPS-MSC = human inducible pluripotent stem cell-derived mesenchymal stem cell.

higher in group 3 than in other groups, significantly higher in group 4 than in groups 1 and 2, but similar between groups 1 and 2. Additionally, IF microscopy demonstrated that the number of γ-H2AX+ cells, an indicator of DNA-damage, displayed an identical pattern to apoptosis among the four groups.

*IHC and IF microscopic findings for identification of the integrity of glomerulus and renal tubules in kidney parenchyma at 72 h after AK-IRI procedure (**Figures 5-8**)*

Microscopy showed that the expression of ZO-1, a tight junction-associated protein, which

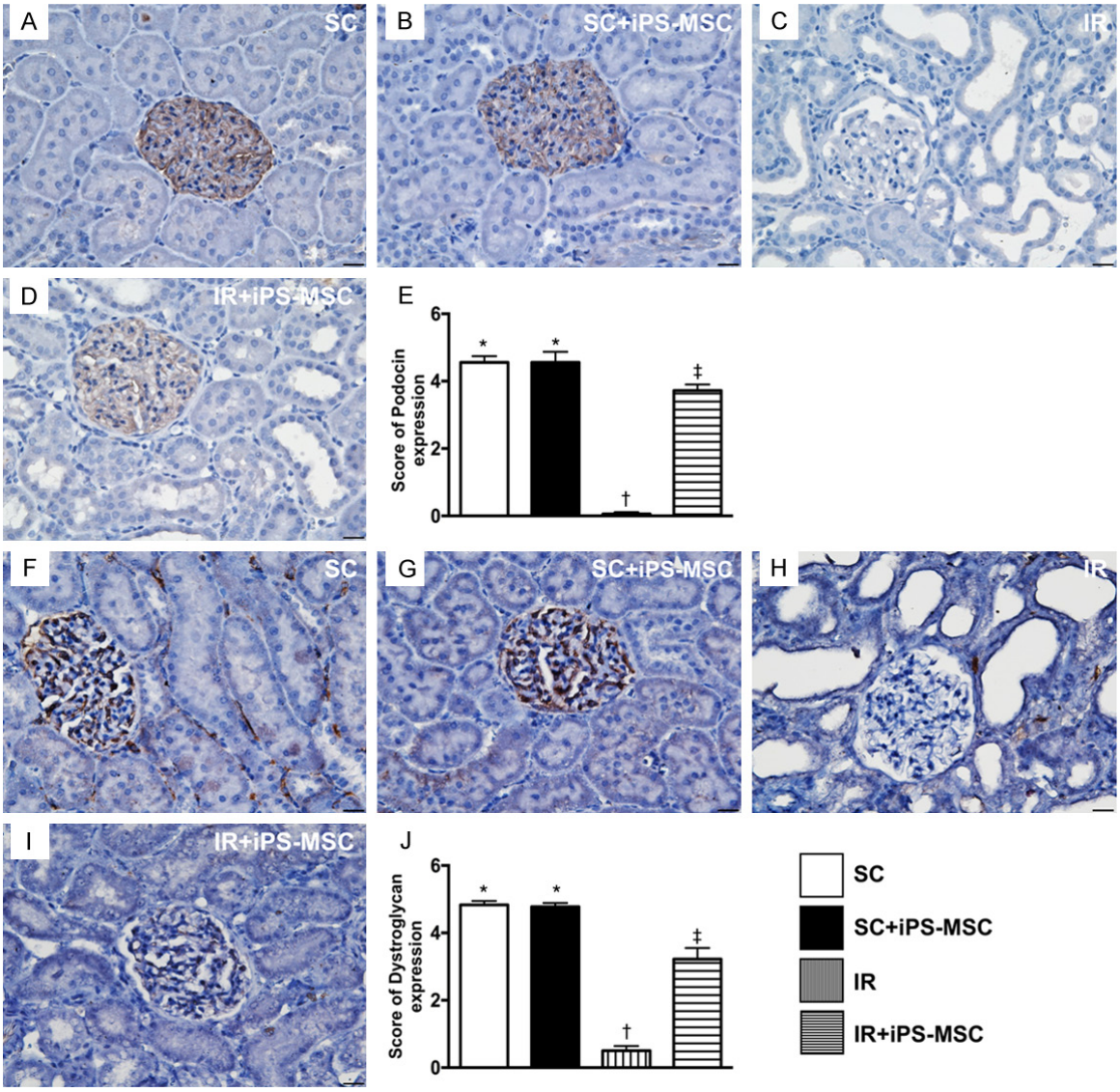

Figure 6. Identification of the expressions of podocin and dystroglycan in glomeruli at day 5 after IR procedure. A-D. Illustrating the microscopic finding (400 ×) of immunohistochemical (IHC) staining for identification of positively-stained podocin in glomerular apparatus (gray color). E. Analytical results of podocin expression, * vs. other groups with different symbols (*, †, ‡), P<0.0001. F-I. Illustrating microscopic findings of IHC staining for identification of positively-stained dystroglycan (400 ×) in glomerular apparatus (gray color). J. Analytical results of dystroglycan expression, * vs. other groups with different symbols (*, †, ‡), P<0.0001. Scale bars in right lower corner represent 20 μm. All statistical analyses were performed by one-way ANOVA, followed by Bonferroni multiple comparison post hoc test (n = 6 for each group). Symbols (*, †, ‡) indicate significance (at 0.05 level). SC = sham control; IR = ischemia reperfusion; iPS-MSC = human inducible pluripotent stem cell-derived mesenchymal stem cell.

provides a link between the integral membrane proteins and the filamentous cytoskeleton in podocytes, was significantly higher in groups 1 and 2 than in groups 3 and 4, and significantly higher in group 4 than in group 3, but it showed no difference between the former two groups (**Figure 5**). The expression of synaptopodin, a component of podocyte foot processes, displayed an identical pattern to ZO-1 among the four groups (**Figure 5**).

Additionally, IHC microscopy demonstrated that the expressions of podocin (**Figure 6**) and dystroglycan (at the base of foot processes; **Figure 6**), two other components of podocyte foot processes, exhibited a similar pattern to ZO-1.

IHC staining revealed change in the expression of P-cadherin (predominantly in the renal glomerulus and colocalized with ZO-1; **Figure 7**), and IF microscopy demonstrated expression of fib-

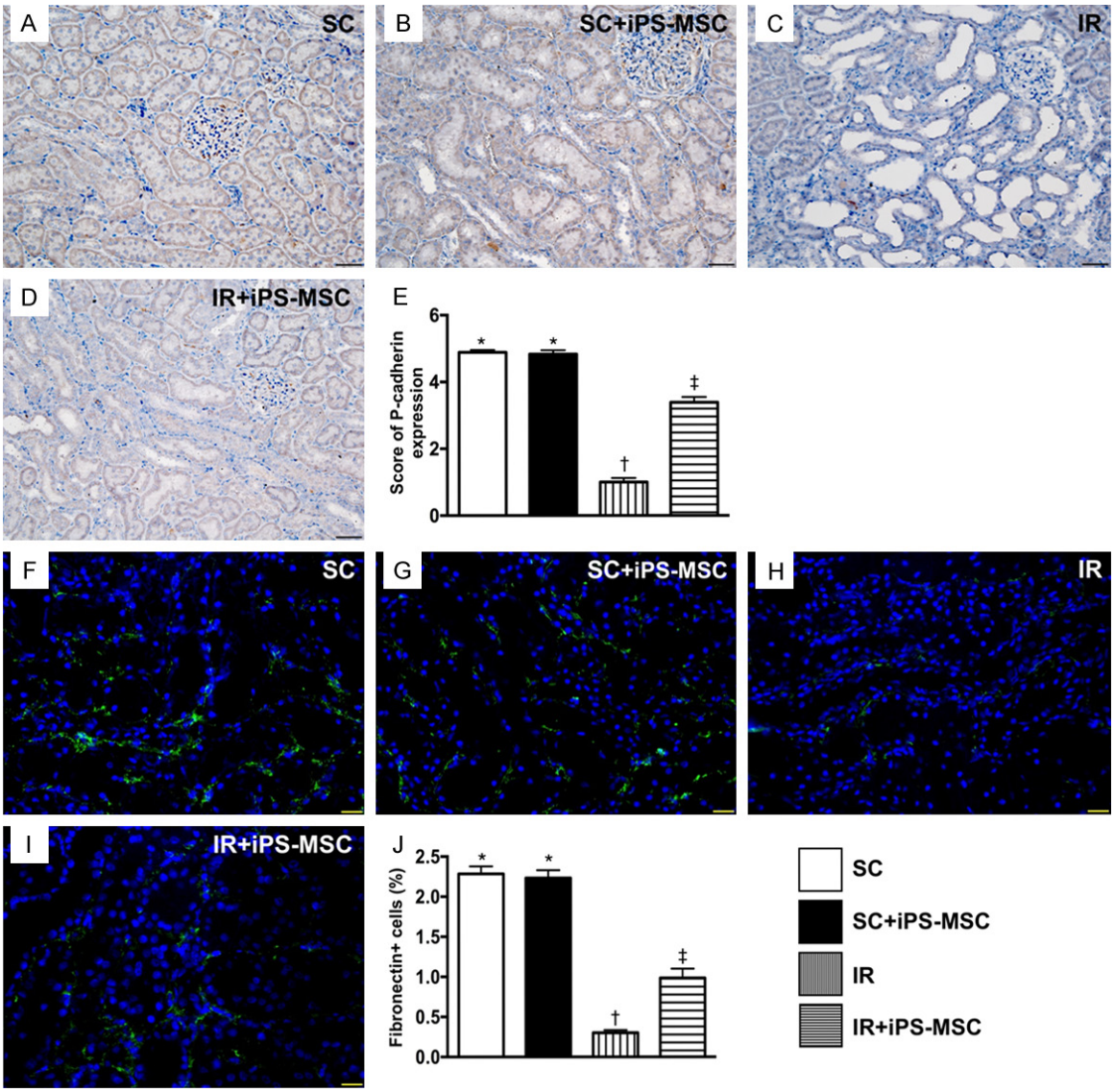

Figure 7. Identification of the expressions of P-cadherin and fibronectin in renal-glomerulus apparatus at day 5 after IR procedure. A-D. Demonstrating microscopic findings (200 ×) from immunohistochemical staining for identification of positively-stained P-cadherin in renal glomerular apparatus (gray color). Scale bars in right lower corner represent 50 μm. E. Analytical results of P-cadherin expression, * vs. other groups with different symbols (*, †, ‡), P<0.0001. F-I. Demonstrating immunofluorescent microscopic findings (400 ×) for identification of positively-stained fibronectin in renal glomerular apparatus (green color). Scale bars in right lower corner represent 20 μm. J. Analytical results of fibronectin expression, * vs. other groups with different symbols (*, †, ‡), P<0.0001. All statistical analyses were performed by one-way ANOVA, followed by Bonferroni multiple comparison post hoc test (n = 6 for each group). Symbols (*, †, ‡) indicate significance (at 0.05 level). SC = sham control; IR = ischemia reperfusion; iPS-MSC = human inducible pluripotent stem cell-derived mesenchymal stem cell.

ronectin in the glomerulus (**Figure 7**), also predominantly in the renal glomerulus, which exhibited an identical pattern to ZO-1 in the four groups.

IF microscopy showed that change in KIM-1, a kidney injury biomarker predominantly expressed in renal tubules, was significantly higher in group 3 than in the other groups, significantly higher in group 4 than groups 1 and 2, but similar between groups 1 and 2 (**Figure 8**). IHC analysis consistently demonstrated that change in the expression of fibroblast specific protein 1 (FSP-1), predominantly situated in the renal interstitial space, showed an identical pattern to that of KIM-1 among the four groups (**Figure 8**).

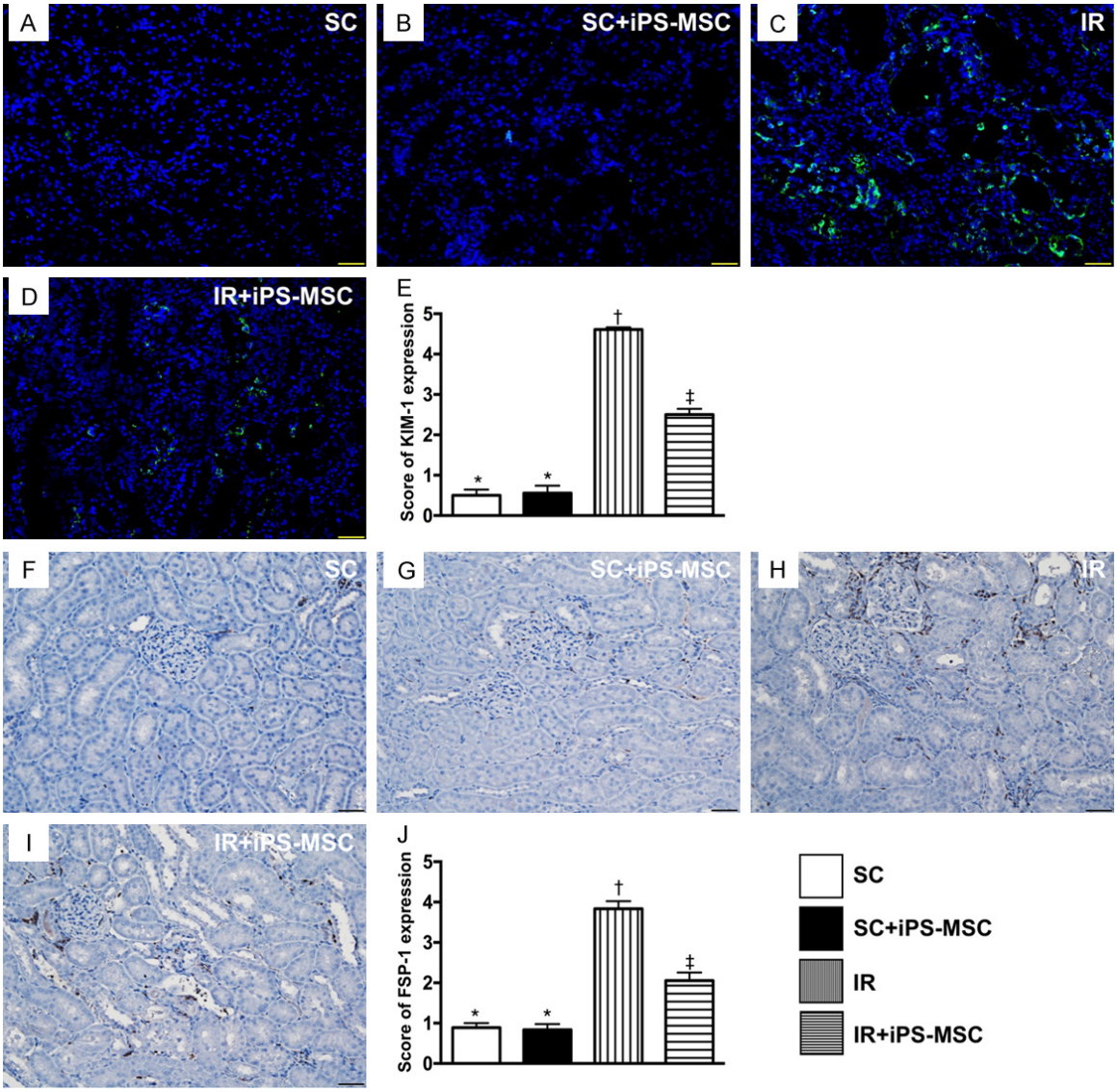

Figure 8. Identification of the expressions of KIM-1 predominantly in renal tubules and FSP-1 predominant in kidney interstitials at day 5 after IR procedure. A-D. Microscopic findings (200 ×) of immunofluorescent staining for identification of kidney injury molecule (KIM)-1 in renal tubules (green color). E. Analytical results of KIM-1 expression, * vs. other groups with different symbols (*, †, ‡), P<0.0001. F-I. Illustrating the microscopic finding (200 ×) of immunofluorescent staining for identification of fibroblast specific protein 1 (FSP-1) predominantly situated in kidney interstitials (gray color). J. Analytical results of FSP-1 expression, * vs. other groups with different symbols (*, †, ‡), P<0.0001. Scale bars in right lower corner represent 50 μm. All statistical analyses were performed by one-way ANOVA, followed by Bonferroni multiple comparison post hoc test (n = 6 for each group). Symbols (*, †, ‡) indicate significance (at 0.05 level). SC = sham control; IR = ischemia reperfusion; iPS-MSC = human inducible pluripotent stem cell-derived mesenchymal stem cell.

Discussion

This study examined the impact of human iPSC-derived MSC therapy on AK-IRI and several striking implications emerged. First, anatomical, molecular and cellular features of kidney parenchyma and renal function as well as the ratio of kidney weight to body weight did not differ between SC animals and SC + iPSC-derived MSC animals, suggesting that human iPSC-derived MSC therapy is safe. Second, as compared with AK-IRI only animals, the renal function and kidney injury score were significantly preserved in AK-IRI animals treated with iPSC-derived MSCs. Third, the molecular-cellular (i.e., inflammation, oxidative stress, apoptosis and glomerulus-renal tubular biomarkers) perturbations were significantly suppressed in

iPSC-derived MSC treated AK-IRI animals than in AK-IRI only animals, highlighting that the cell therapy effectively preserved kidney parenchyma from AK-IRI injury.

While abundant data have shown that MSC therapies, especially adipose-derived MSC therapies, significantly protected against AK-IRI [18, 20, 33, 34], research investigating the therapeutic impact of human iPSC-derived MSC on AK-IRI is lacking [35-37]. The most important finding in the present study was that the circulating levels of creatinine and BUN, the ratio of urine protein to creatinine (i.e., indices of renal function), the ratio of kidney weight to body weight (i.e., indicator of gross anatomy), and kidney injury score (i.e., indicates histopathological finding) were significantly higher in AK-IRI animals than in SC animals, and were significantly reduced in iPSC-derived MSC treated AK-IRI animals. Importantly, no side effects of iPSC-derived MSC therapy were found in SC or AK-IRI animals after receiving iPSC-derived MSC therapy. Our findings strengthen those of previous studies [35-37] and highlight that iPSC-derived MSC therapy was safe and efficacious for animals with AK-IRI.

The essential findings in the present study were that, as compared with SC group, the inflammation, oxidative stress, cellular apoptosis and DNA damaged biomarkers were substantially augmented in the AK-IRI group. Of importance was that these molecular-cellular perturbations were alleviated in AK-IRI animals after receiving iPSC-derived MSC therapy. These findings could partially explain why renal function was preserved and kidney injury score was ameliorated in AK-IRI animals treated by iPSC-derived MSCs.

The kidney is vulnerable to damage in various disease states [3-8, 10-14]. The present study indicated that glomerular and renal tubular architectures, and the integrity of podocyte components, were devastated in AK-IRI animals compared to SC animals, which is consistent with previous studies [3-8, 10-14]. The present study distinctly demonstrated that the architectures of glomeruli, renal tubules and podocyte components were preserved in AK-IRI animals treated by iPSC-derived MSCs. These findings could again explain why the kidney injury score and proteinuria were markedly attenuated in animals treated by iPSC-derived MSCs.

Although the angiogenesis capacity of MSCs is believed to be inferior to endothelial progenitor cells, this capacity in adipose-derived MSCs has been clearly identified by previous studies [18, 20]. Consistent with previous studies [18, 20], we found that iPSC-derived MSC therapy restored endothelial cell markers (i.e., CD31, vWF) and enhanced the expression of angiogenesis biomarkers in kidney parenchyma. Our findings again indicated that renal function was preserved by iPSC-derived MSC therapy, possibly through restoring microvasculature and/or blood flow in the IRI-injured kidney.

Study limitations

This study has limitations. First, although the results of the present study were promising, the study period was only for 72 h, so the long-term effects of iPSC-derived MSC therapy for AK-IRI remains uncertain. Second, the possibility of tumorigenesis is outside the scope of this study.

In conclusion, the present study demonstrated that iPSC-derived MSC therapy appears safe and effective for preserving renal function and the integrity of kidney parenchyma in rodents in the setting of AK-IRI.

Acknowledgements

This study was supported by a program grant from Chang Gung Memorial Hospital, Chang Gung University (Grant number: CMRPG8F1721).

Disclosure of conflict of interest

None.

Address correspondence to: Dr. Hon-Kan Yip, Division of Cardiology, Department of Internal Medicine, Kaohsiung Chang Gung Memorial Hospital and Chang Gung University College of Medicine, Kaohsiung 83301, Taiwan. Tel: +886-7-7317123; Fax: +886-7-7322402; E-mail: han.gung@msa.hinet.net; Dr. Chih-Chao Yang, Division of Nephrology, Department of Internal Medicine, Kaohsiung Chang Gung Memorial Hospital and Chang Gung University College of Medicine, Kaohsiung 83301, Taiwan. Tel: +886-7-7317123; Fax: +886-7-732-2402; E-mail: papaofison@gmail.com

References

[1] Pickering JW, James MT and Palmer SC. Acute kidney injury and prognosis after cardiopulmo-

nary bypass: a meta-analysis of cohort studies. Am J Kidney Dis 2015; 65: 283-293.
[2] Rossaint J and Zarbock A. Acute kidney injury: definition, diagnosis and epidemiology. Minerva Urol Nefrol 2016; 68: 49-57.
[3] Awdishu L. Drug-induced kidney disease in the ICU: mechanisms, susceptibility, diagnosis and management strategies. Curr Opin Crit Care 2017; 23: 484-490.
[4] Kaltsas E, Chalikias G and Tziakas D. The incidence and the prognostic impact of acute kidney injury in acute myocardial infarction patients: current preventive strategies. Cardiovasc Drugs Ther 2018; 32: 81-98.
[5] Kimmel LA, Wilson S, Walker RG, Singer Y and Cleland H. Acute kidney injury: it's not just the 'big' burns. Injury 2018; 49: 213-218.
[6] Hoste EAJ and Vandenberghe W. Epidemiology of cardiac surgery-associated acute kidney injury. Best Pract Res Clin Anaesthesiol 2017; 31: 299-303.
[7] Kristovic D, Horvatic I, Husedzinovic I, Sutlic Z, Rudez I, Baric D, Unic D, Blazekovic R and Crnogorac M. Cardiac surgery-associated acute kidney injury: risk factors analysis and comparison of prediction models. Interact Cardiovasc Thorac Surg 2015; 21: 366-373.
[8] Xu J, Jiang W, Shen B, Fang Y, Teng J, Wang Y and Ding X. Acute kidney injury in cardiac surgery. Contrib Nephrol 2018; 193: 127-136.
[9] Inohara T, Numasawa Y, Higashi T, Ueda I, Suzuki M, Hayashida K, Yuasa S, Maekawa Y, Fukuda K and Kohsaka S. Predictors of high cost after percutaneous coronary intervention: a review from Japanese multicenter registry overviewing the influence of procedural complications. Am Heart J 2017; 194: 61-72.
[10] Ram P, Mezue K, Pressman G and Rangaswami J. Acute kidney injury post-transcatheter aortic valve replacement. Clin Cardiol 2017; 40: 1357-1362.
[11] Shendi AM, Wallis G, Painter H, Harber M and Collier S. Epidemiology and impact of bloodstream infections among kidney transplant recipients: a retrospective single-center experience. Transpl Infect Dis 2018; 20.
[12] Kotecha A, Vallabhajosyula S, Coville HH and Kashani K. Cardiorenal syndrome in sepsis: a narrative review. J Crit Care 2018; 43: 122-127.
[13] Friedericksen DV, Van der Merwe L, Hattingh TL, Nel DG and Moosa MR. Acute renal failure in the medical ICU still predictive of high mortality. S Afr Med J 2009; 99: 873-875.
[14] Sementilli A and Franco M. Renal acute cellular rejection: correlation between the immunophenotype and cytokine expression of the inflammatory cells in acute glomerulitis, arterial intimitis, and tubulointerstitial nephritis. Transplant Proc 2010; 42: 1671-1676.
[15] Ali T, Khan I, Simpson W, Prescott G, Townend J, Smith W and Macleod A. Incidence and outcomes in acute kidney injury: a comprehensive population-based study. J Am Soc Nephrol 2007; 18: 1292-1298.
[16] Xue JL, Daniels F, Star RA, Kimmel PL, Eggers PW, Molitoris BA, Himmelfarb J and Collins AJ. Incidence and mortality of acute renal failure in Medicare beneficiaries, 1992 to 2001. J Am Soc Nephrol 2006; 17: 1135-1142.
[17] Boros P and Bromberg JS. New cellular and molecular immune pathways in ischemia/reperfusion injury. Am J Transplant 2006; 6: 652-658.
[18] Chen YT, Sun CK, Lin YC, Chang LT, Chen YL, Tsai TH, Chung SY, Chua S, Kao YH, Yen CH, Shao PL, Chang KC, Leu S and Yip HK. Adipose-derived mesenchymal stem cell protects kidneys against ischemia-reperfusion injury through suppressing oxidative stress and inflammatory reaction. J Transl Med 2011; 9: 51.
[19] El Eter EA and Aldrees A. Inhibition of proinflammatory cytokines by SCH79797, a selective protease-activated receptor 1 antagonist, protects rat kidney against ischemia-reperfusion injury. Shock 2012; 37: 639-644.
[20] Sung PH, Chiang HJ, Wallace CG, Yang CC, Chen YT, Chen KH, Chen CH, Shao PL, Chen YL, Chua S, Chai HT, Chen YL, Huang TH, Yip HK and Lee MS. Exendin-4-assisted adipose derived mesenchymal stem cell therapy protects renal function against co-existing acute kidney ischemia-reperfusion injury and severe sepsis syndrome in rat. Am J Transl Res 2017; 9: 3167-3183.
[21] Chang CL, Sung PH, Sun CK, Chen CH, Chiang HJ, Huang TH, Chen YL, Zhen YY, Chai HT, Chung SY, Tong MS, Chang HW, Chen HH and Yip HK. Protective effect of melatonin-supported adipose-derived mesenchymal stem cells against small bowel ischemia-reperfusion injury in rat. J Pineal Res 2015; 59: 206-220.
[22] Chen HH, Lin KC, Wallace CG, Chen YT, Yang CC, Leu S, Chen YC, Sun CK, Tsai TH, Chen YL, Chung SY, Chang CL and Yip HK. Additional benefit of combined therapy with melatonin and apoptotic adipose-derived mesenchymal stem cell against sepsis-induced kidney injury. J Pineal Res 2014; 57: 16-32.
[23] Chen YT, Chiang HJ, Chen CH, Sung PH, Lee FY, Tsai TH, Chang CL, Chen HH, Sun CK, Leu S, Chang HW, Yang CC and Yip HK. Melatonin treatment further improves adipose-derived mesenchymal stem cell therapy for acute interstitial cystitis in rat. J Pineal Res 2014; 57: 248-261.
[24] Sun CK, Yen CH, Lin YC, Tsai TH, Chang LT, Kao YH, Chua S, Fu M, Ko SF, Leu S and Yip HK. Autologous transplantation of adipose-derived mesenchymal stem cells markedly reduced

acute ischemia-reperfusion lung injury in a rodent model. J Transl Med 2011; 9: 118.
[25] Maumus M, Guerit D, Toupet K, Jorgensen C and Noel D. Mesenchymal stem cell-based therapies in regenerative medicine: applications in rheumatology. Stem Cell Res Ther 2011; 2: 14.
[26] Sun L, Wang D, Liang J, Zhang H, Feng X, Wang H, Hua B, Liu B, Ye S, Hu X, Xu W, Zeng X, Hou Y, Gilkeson GS, Silver RM, Lu L and Shi S. Umbilical cord mesenchymal stem cell transplantation in severe and refractory systemic lupus erythematosus. Arthritis Rheum 2010; 62: 2467-2475.
[27] Thum T, Bauersachs J, Poole-Wilson PA, Volk HD and Anker SD. The dying stem cell hypothesis: immune modulation as a novel mechanism for progenitor cell therapy in cardiac muscle. J Am Coll Cardiol 2005; 46: 1799-1802.
[28] Focosi D and Amabile G. Induced pluripotent stem cell-derived red blood cells and platelet concentrates: from bench to bedside. Cells 2017; 7.
[29] Magli A and Perlingeiro RR. Myogenic progenitor specification from pluripotent stem cells. Semin Cell Dev Biol 2017; 72: 87-98.
[30] Salas S, Ng N, Gerami-Naini B and Anchan RM. Induced pluripotent stem cells from ovarian tissue. Curr Protoc Hum Genet 2017; 95: 21.10.1-21.10.22.
[31] Singh Dolt K, Hammachi F and Kunath T. Modeling Parkinson's disease with induced pluripotent stem cells harboring alpha-synuclein mutations. Brain Pathol 2017; 27: 545-551.
[32] Chhabra A. Derivation of human induced pluripotent stem cell (iPSC) lines and mechanism of pluripotency: historical perspective and recent advances. Stem Cell Rev 2017; 13: 757-773.
[33] Chen CH, Cheng BC, Chen KH, Shao PL, Sung PH, Chiang HJ, Yang CC, Lin KC, Sun CK, Sheu JJ, Chang HW, Lee MS and Yip HK. Combination therapy of exendin-4 and allogenic adipose-derived mesenchymal stem cell preserved renal function in a chronic kidney disease and sepsis syndrome setting in rats. Oncotarget 2017; 8: 100002-100020.
[34] Lin KC, Yip HK, Shao PL, Wu SC, Chen KH, Chen YT, Yang CC, Sun CK, Kao GS, Chen SY, Chai HT, Chang CL, Chen CH and Lee MS. Combination of adipose-derived mesenchymal stem cells (ADMSC) and ADMSC-derived exosomes for protecting kidney from acute ischemia-reperfusion injury. Int J Cardiol 2016; 216: 173-185.
[35] Imberti B, Tomasoni S, Ciampi O, Pezzotta A, Derosas M, Xinaris C, Rizzo P, Papadimou E, Novelli R, Benigni A, Remuzzi G and Morigi M. Renal progenitors derived from human iPSCs engraft and restore function in a mouse model of acute kidney injury. Sci Rep 2015; 5: 8826.
[36] Li Q, Tian SF, Guo Y, Niu X, Hu B, Guo SC, Wang NS and Wang Y. Transplantation of induced pluripotent stem cell-derived renal stem cells improved acute kidney injury. Cell Biosci 2015; 5: 45.
[37] Toyohara T, Mae S, Sueta S, Inoue T, Yamagishi Y, Kawamoto T, Kasahara T, Hoshina A, Toyoda T, Tanaka H, Araoka T, Sato-Otsubo A, Takahashi K, Sato Y, Yamaji N, Ogawa S, Yamanaka S and Osafune K. Cell therapy using human induced pluripotent stem cell-derived renal progenitors ameliorates acute kidney injury in mice. Stem Cells Transl Med 2015; 4: 980-992.

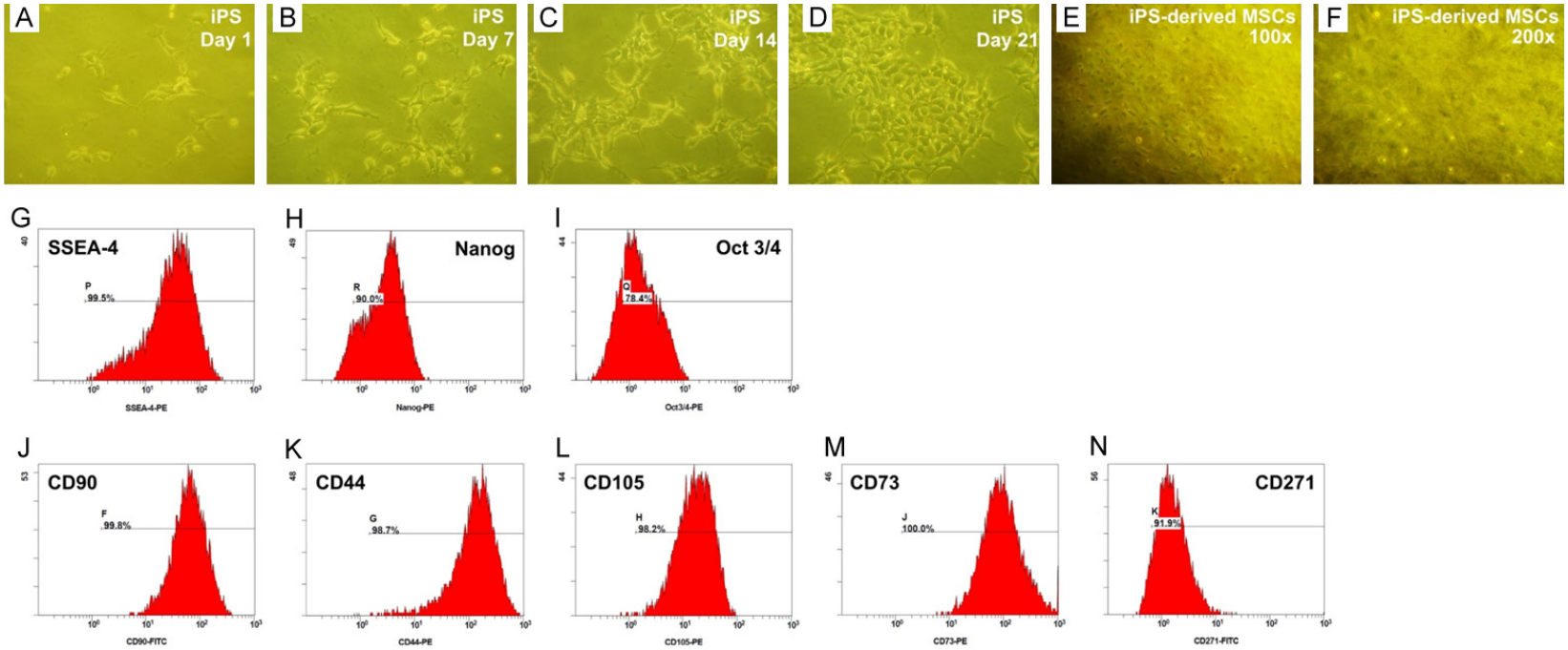

Supplementary Figure 1. Illustrating that human inducible pluripotent stem cells (iPSC) differentiated into mesenchymal stem cells (MSCs). Upper panel: (A-D) Microscopic findings (200 ×) at different time courses (i.e., at days 1, 7, 14 and 21) for culturing iPSC, showing morphology and colony. (E and F) Microscopy (100 × and 200 ×, respectively) showing morphologic features of iPS-derived MSCs (i.e. P2 cells ready for subculture). Middle panel: (G-I) Illustrating flow cytometric analyses for identification of iPS specific surface markers (i.e., SSEA-4, Nanog, and Oct3/4). Lower panel: (J-N) Showing flow cytometric analyses for identifying iPS-derived MSC specific surface markers, i.e., high population of CD90+, CD44+, CD105+, CD73+, and CD217+ cell surface makers.

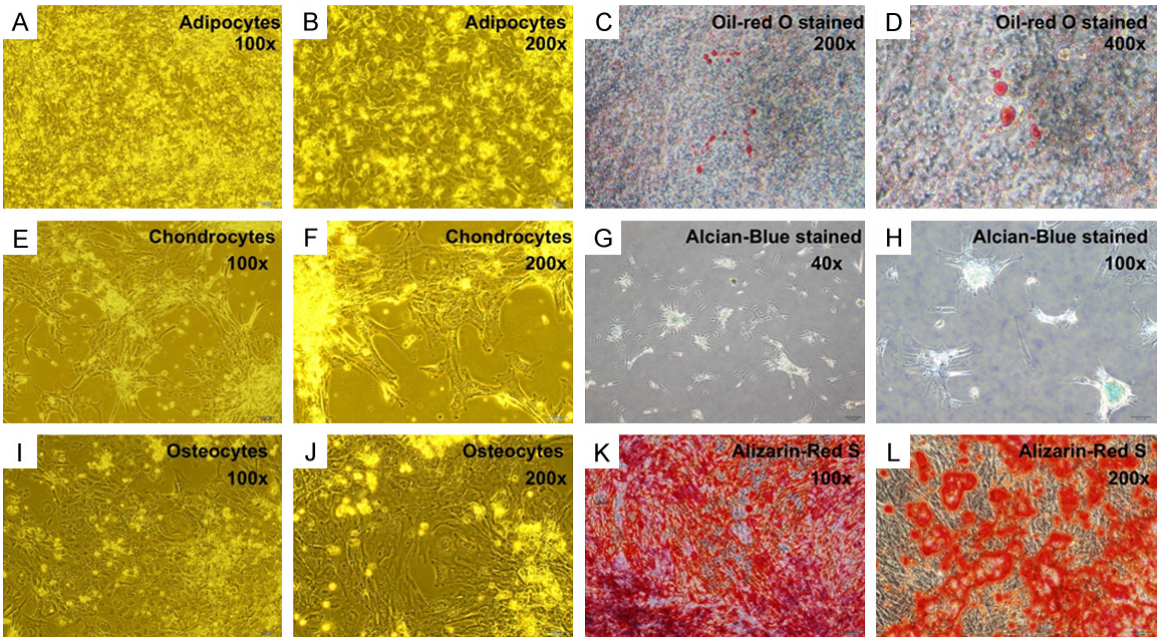

Supplementary Figure 2. Illustrating cell-culture results of iPSC derived MSCs differentiated into adipocytes, chondrocytes and osteocytes. A and B. Microscopic findings (100 ×, 200 ×) for culturing matured adipocytes derived from iPS-MSC (i.e., adipogenic differentiation). C and D. Microscopic findings (200 ×, 400 ×) of positively oil-red O stained adipocytes. E and F. Microscopic findings (100 ×, 200 ×) of culturing matured chondrocytes derived from iPS-MSC (i.e., chondrogenic differentiation). G, H. Microscopic findings (40 ×, 100 ×) for positively Alcian-Blue stained chondrocytes. I and J. Microscopic findings (100 ×, 200 ×) for culturing matured osteocytes derived from iPS-MSC (i.e., osteogenic differentiation). K, L. Microscopic findings (100 ×, 200 ×) of positively Alizarin-Red S stained osteocytes.

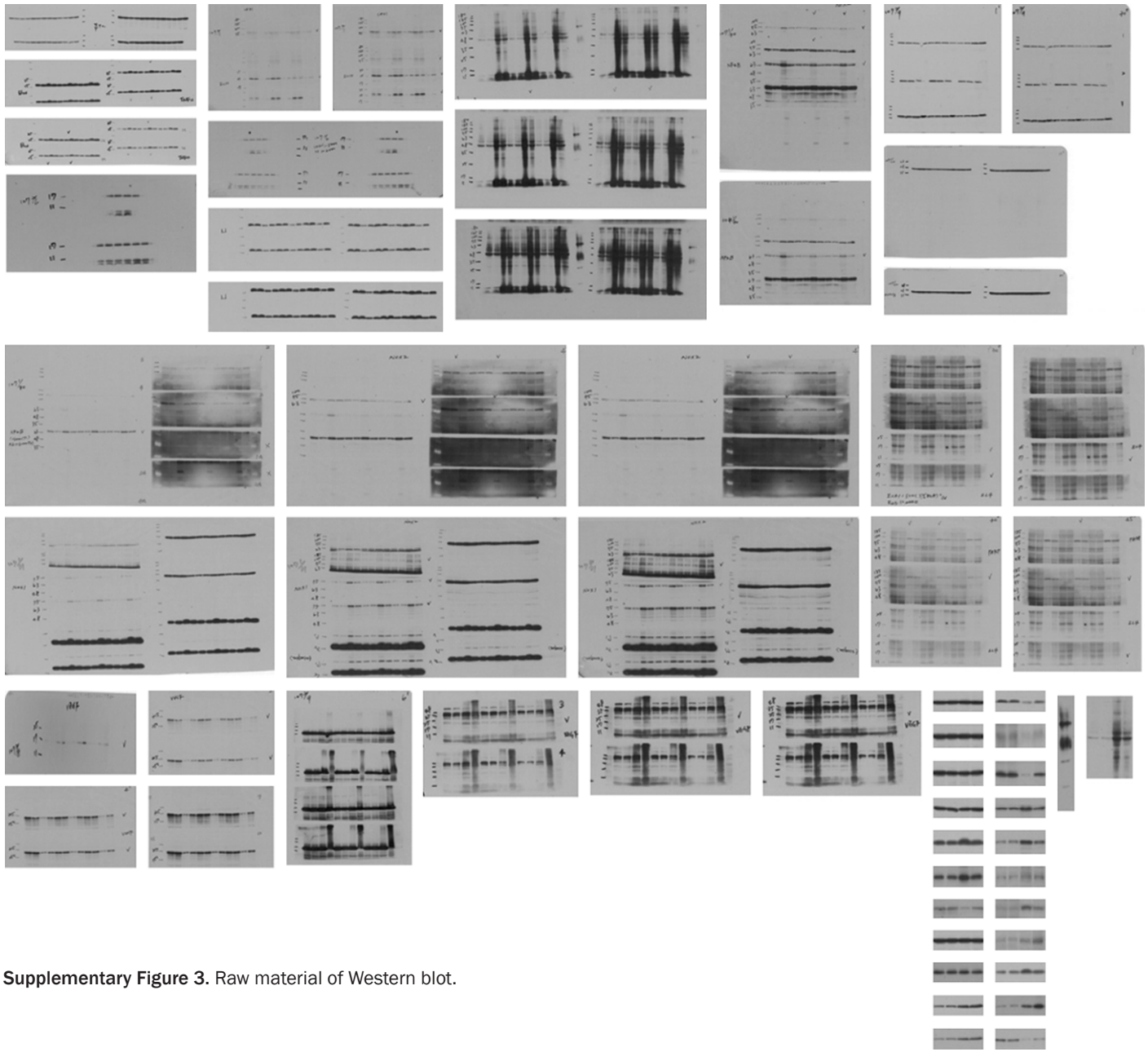

Supplementary Figure 3. Raw material of Western blot.